

*Citation for published version:*

Coles, N, Mahon, M & Webster, R 2017, 'Phosphine- and Amine-Borane Dehydrocoupling Using a Three Coordinate Iron(II) -Diketiminato Pre-Catalyst', *Organometallics*, vol. 36, no. 11, pp. 2262-2268.  
<https://doi.org/10.1021/acs.organomet.7b00326>

*DOI:*

[10.1021/acs.organomet.7b00326](https://doi.org/10.1021/acs.organomet.7b00326)

*Publication date:*

2017

*Document Version*

Peer reviewed version

[Link to publication](https://doi.org/10.1021/acs.organomet.7b00326)

This document is the Accepted Manuscript version of a Published Work that appeared in final form in *Organometallics*, copyright © American Chemical Society, after peer review and technical editing by the publisher. To access the final edited and published work see <https://doi.org/10.1021/acs.organomet.7b00326>.

**University of Bath**

## **Alternative formats**

If you require this document in an alternative format, please contact:  
[openaccess@bath.ac.uk](mailto:openaccess@bath.ac.uk)

### **General rights**

Copyright and moral rights for the publications made accessible in the public portal are retained by the authors and/or other copyright owners and it is a condition of accessing publications that users recognise and abide by the legal requirements associated with these rights.

### **Take down policy**

If you believe that this document breaches copyright please contact us providing details, and we will remove access to the work immediately and investigate your claim.

# Phosphine- and Amine-Borane Dehydrocoupling

## Using a Three Coordinate Iron(II) $\beta$ -Diketimate

### Pre-Catalyst

*Nathan T. Coles, Mary F. Mahon and Ruth L. Webster\**

Department of Chemistry, University of Bath, Claverton Down, Bath, United Kingdom. BA2 7AY.

**ABSTRACT** Dehydrocoupling of phosphine- and amine-boranes is reported using an iron(II)  $\beta$ -diketimate complex. Dehydrocoupling of amine-boranes is far more facile than the phosphine counterpart, the former proceeding at room temperature with 1 mol% iron pre-catalyst. This low loading is sufficient to allow *in situ* kinetic analysis and deuterium labeling studies to take place. An iron amido-borane complex has also been isolated, which is believed to be the catalyst resting state. Overall, this has allowed us to postulate a catalytic cycle which proceeds *via* release of diborazane and iron hydride and iron amido-borane intermediates.

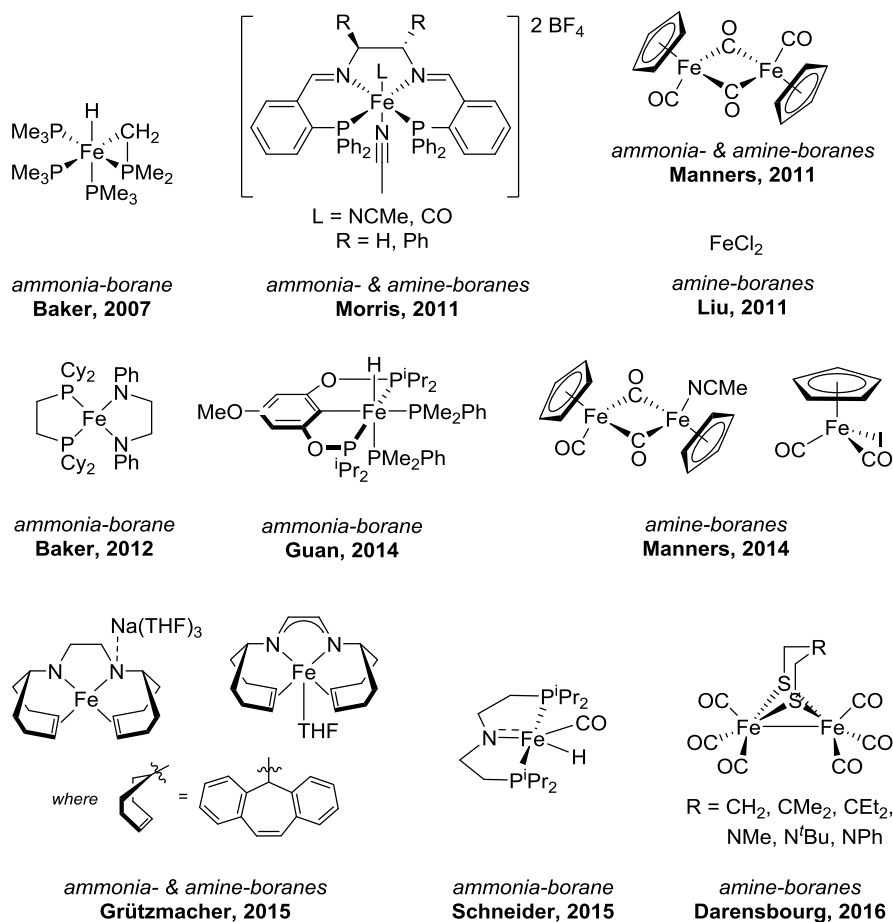
**KEYWORDS** Iron, homogeneous catalysis, dehydrocoupling, dehydropolymerization, phosphine-boranes, amine-boranes.

### INTRODUCTION

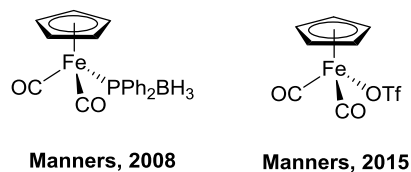
Dehydrocoupling of main group compounds is a powerful tool in sustainable catalysis. For example, the dehydrocoupling of ammonia-borane ( $\text{NH}_3 \cdot \text{BH}_3$ ), due to the high yield of  $\text{H}_2$  that can

be produced relative to the molecular weight of the starting material, means it has the potential to be an efficient and atom economic method of H<sub>2</sub> storage.<sup>1-20</sup> Dehydrocoupling of other main group substrates containing diverse functionality (particularly focusing on other amine- and phosphine-boranes) not only provide an alternative to ammonia-borane but can be used to synthesize novel main group compounds or, with judicious selection of substrate, can be used to prepare main group polymers.<sup>21-36</sup> Alternatively, they proffer excellent opportunities for mechanistic study<sup>32</sup> with which new dehydrocoupling catalysis can be developed. In the context of sustainable chemical bond transformations, iron catalysis provides an exceptional opportunity to address many of the challenges of green chemistry, but it is surprising to note that only recently have a handful of iron complexes have been reported for amine-borane dehydrocoupling<sup>37-49</sup> and fewer still for phosphine-borane dehydrocoupling (Figure 1).<sup>50, 51</sup> It has already been shown that simple, three-coordinate iron(II)  $\beta$ -diketiminates.<sup>52-55</sup> are highly tunable complexes, undertaking a range of catalytic transformations.<sup>56-64</sup> With this in mind, we sought to develop dehydrocoupling to tackle a diverse selection of phosphine- and amine-borane substrates whilst using a well-defined pre-catalyst to produce a detailed mechanistic investigation of (alkyl)amine-borane dehydrocoupling reactivity.<sup>44, 46</sup>

### Amine-borane dehydrocoupling pre-catalysts



### Phosphine-borane dehydrocoupling pre-catalysts



### This work

#### Phosphine- and amine-borane dehydrocoupling

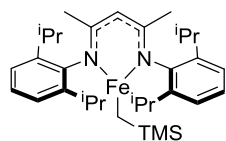
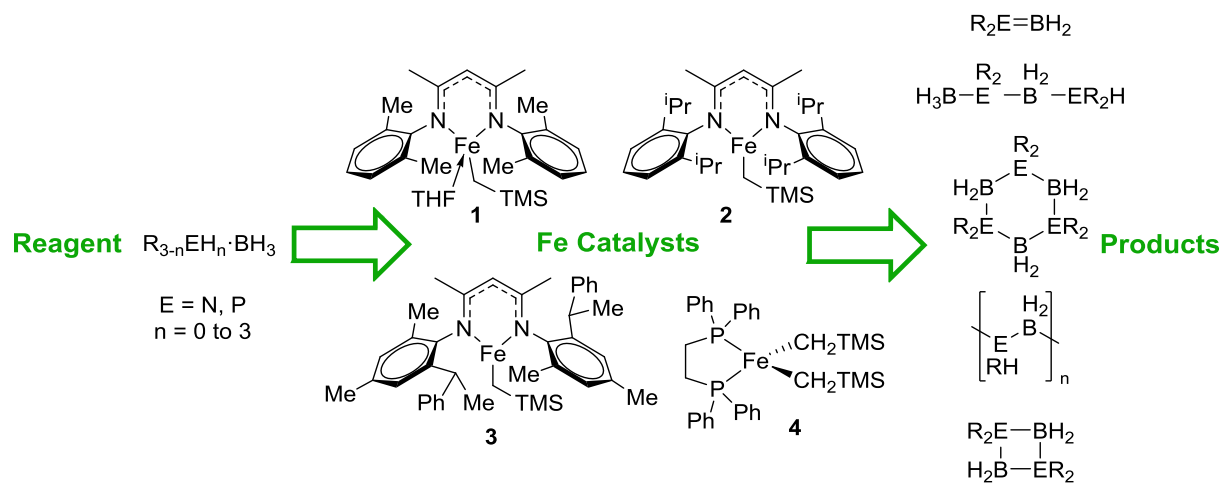


**Figure 1.** Current examples of discrete iron complexes prepared and implemented in ammonia-, amine- and phosphine-borane dehydrocoupling.

## RESULTS AND DISCUSSION

We initiated our studies by testing three  $\beta$ -diketiminato complexes in phosphine-borane dehydrocoupling (**1-3**, E = P, Scheme 1). The fourth complex (**4**) has been shown by Chirik to effect olefin polymerization<sup>65</sup> and contains the same labile  $\text{CH}_2\text{TMS}$  co-ligand as complexes **1** to **3**.



**Scheme 1.** Fe(II) pre-catalysts used to catalyze the dehydrocoupling of phosphine- and amine-boranes.

The 2,6-dimethyl complex, **1**, gives some dehydrocoupled product **5b** after 24 h at 90 °C (Table 1, Entry 1), changing to the slightly more bulky 2,6-diisopropyl congener, **2**, results in an increase in yield of **5b** to 52% under the same reaction conditions (Entry 2). A further change in substitution pattern to complex **3** does not increase the yield. Presumably in this instance steric bulk around the iron center is limiting. Pre-catalyst **4** does not give good levels of dehydrocoupling and only 36% **5b** is obtained (Entry 4). This may be unsurprising based on reports from Baker and co-workers on the dehydrocoupling of ammonia-borane where the authors noted that, when using the iron phosphine complex  $\text{FeH}(\text{PMe}_2\text{CH}_2)(\text{PMe}_3)_3$  although there was evidence for dehydrocoupling

taking place, a black precipitate also formed which was not catalytically active.<sup>37</sup> The <sup>11</sup>B NMR spectrum recorded also showed the formation of Me<sub>3</sub>P·BH<sub>3</sub>, indicative of catalyst decomposition in the presence of borane-substrate. This is similar to our own observations with pre-catalyst **4** in the presence of Ph<sub>2</sub>HP·BH<sub>3</sub> where new phosphine-borane adducts are observed by <sup>11</sup>B NMR, believed to be ligand-borane adducts.

Using pre-catalyst **2**, we proceeded to optimize the reaction conditions further, finding that 10 mol% **2** and heating to 110 °C gives selective formation of **5a** (Entries 7 and 8). For comparison, the non-catalyzed reaction requires heating to 170 °C to generate **5a** and cyclic tetramer ((Ph<sub>2</sub>P–BH<sub>2</sub>)<sub>4</sub>) in an 8 : 1 ratio.<sup>66</sup>

**Table 1.** Optimization of dehydrocoupling using Ph<sub>2</sub>HP·BH<sub>3</sub> as the standard substrate.

Entry	Catalyst (loading, mol%)	Conditions	Spec. Yield (%) <sup>a</sup>	<b>5a</b> : <b>5b</b>
1	<b>1</b> (5)	90 °C, 24 h, C <sub>6</sub> D <sub>6</sub>	30	0 : 1
2	<b>2</b> (5)	90 °C, 24 h, C <sub>6</sub> D <sub>6</sub>	52	0 : 1
3	<b>3</b> (5)	90 °C, 24 h, C <sub>6</sub> D <sub>6</sub>	43	0 : 1
4	<b>4</b> (5)	90 °C, 24 h, C <sub>6</sub> D <sub>6</sub>	36	0 : 1
5	<b>2</b> (10)	90 °C, 72 h, C <sub>6</sub> D <sub>6</sub>	89	1 : 1.5
6	<b>2</b> (5)	110 °C, 72 h, toluene	94	3.3 : 1
7	<b>2</b> (10)	110 °C, 72 h, toluene	98	1 : 0
8	<b>2</b> (10)	110 °C, 36 h, toluene	95	1 : 0

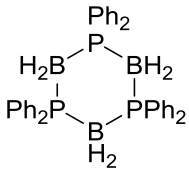
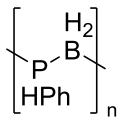
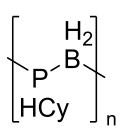
Conditions: Ph<sub>2</sub>HP·BH<sub>3</sub> (0.25 mmol), solvent (0.5 mL), argon atmosphere.  
<sup>a</sup>Spectroscopic yield obtained by NMR: <sup>31</sup>P NMR set with a 50 second relaxation delay and referenced to H<sub>3</sub>PO<sub>4</sub>.

Exploring the substrate scope with phosphine boranes shows a large dependency on phosphines with phenyl substitution (Table 2, compare Entries 1 and 2). Formation of poly(phosphine-boranes) is successful and the precipitate of both the high molecular weight (toluene insoluble) fraction and the lower molecular weight (toluene soluble fraction) could be separated and analyzed by GPC (Entry 3). For comparison, Manners achieved  $M_n$  59 kDa and PDI 1.6 using only 1 mol%  $\text{Cp}(\text{CO})_2\text{Fe}(\text{OTf})$  at 100 °C for 24 h, whereas the more coordinating iodide adduct,  $\text{Cp}(\text{CO})_2\text{FeI}$ , gave  $M_n$  18 kDa after 24 h at 100 °C and required 10 mol% catalyst loading.<sup>51</sup> So although **2** is not competitive with  $\text{Cp}(\text{CO})_2\text{Fe}(\text{OTf})$  it is interesting that Manners' change in counter ion leads to such a vast change in activity and is a potential area for future research in the context of this study. Although a small amount of high molecular weight species is obtained using cyclohexylphosphine-borane (Entry 4), this product could not be precipitated from the crude reaction mixture and was analyzed as a mixture with the low molecular oligomers which form the major reaction product (see Supporting Information page 38, for GPC spectrum). Both phenyl- and cyclohexylphosphine-borane polymerizations were run until the starting material was completely consumed. Worthy of note in this respect is Manners and Scheer's elegant metal-free route to poly(phosphine-boranes) from the corresponding Lewis base stabilized phosphine-borane monomer, which gives access to otherwise challenging to prepare alkyl-substituted products with high  $M_n$  and moderate PDI.<sup>67</sup>

Understanding the mechanism of phosphine-borane dehydrocoupling *via* kinetic analysis is not trivial because of the paramagnetism encountered at fairly high iron loadings. However, preliminary studies are possible. By using the dehydrocoupling of  $\text{Ph}_2\text{HP}\cdot\text{BH}_3$  as the model reaction, addition of a sub-catalytic amount of  $\text{PMe}_3$  to the reaction mixture does not result in suppression of the formation of **5a**. If the reaction was heterogeneous, and iron nanoparticles were present, the addition of a small quantity of phosphine would block the active sites and slow or

prevent catalytic turnover.<sup>68</sup> Over the standard reaction period for this substrate, 99% **5a** forms. The thermal reaction in the absence of catalyst and PMe<sub>3</sub> results in 39% **5b**. We therefore postulate that low levels of non-catalytic dehydrocoupling take place to form the dimeric product, but the presence of catalyst increases the yield of this species. The formation of **5a** under our standard reaction conditions is iron mediated and this appears to be a homogeneous process. Use of TEMPO as a radical trap or iodo(methyl)cyclopropane as a radical clock does not suppresses the formation of **5a** (99% **5a** after 36 h in the presence of TEMPO at 110 °C with 10 mol% **2**), suggesting that the iron catalyzed aspects are not radical mediated.

**Table 2.** Phosphine-borane dehydrocoupling substrate scope, catalyzed by **2**.

Entry	Substrate	Product	<sup>31</sup> P NMR Chemical Shift, ppm (multiplicity) <sup>a</sup>	Spec. Yield, % <sup>b</sup>	GPC Data
1	Ph <sub>2</sub> HP·BH <sub>3</sub>		-16.6 (br. s)	<b>5a</b> 95	N/A
2	Cy <sub>2</sub> HP·BH <sub>3</sub>	Cy <sub>2</sub> HP·BH <sub>2</sub> -Cy <sub>2</sub> P·BH <sub>3</sub>	16.4 (d), -12.2 (s)	<b>5c</b> < 10	N/A
3 <sup>c,d</sup>	PhH <sub>2</sub> P·BH <sub>3</sub>		-46.5 to -58.0 (br. s)	<b>5d</b> 61%	M <sub>n</sub> 55.0 kDa PDI 1.9
4 <sup>d</sup>	CyH <sub>2</sub> P·BH <sub>3</sub>		-33.5 to -42.2 (br. s)	<b>5e</b> <10%	M <sub>n</sub> 54.6 kDa PDI 1.3

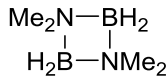
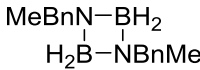
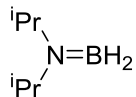
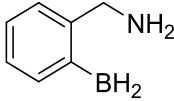
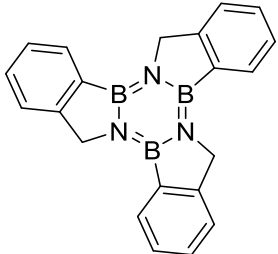
Conditions: Phosphine-borane (0.25 mmol), **2** (14 mg, 10 mol%), toluene (0.5 mL), 110 °C, argon atmosphere. All 72 h except Entry 1 (36 h). <sup>a</sup>Multiplicity expressed as br. = broad, s = singlet, d = doublet, see supporting information for <sup>11</sup>B NMR data and associated spectra. <sup>b</sup>Spectroscopic yield obtained by NMR: <sup>31</sup>P NMR set with a 50 second relaxation delay referenced to H<sub>3</sub>PO<sub>4</sub>. <sup>c</sup>6



mol% **2**. Isolated yield of polymer precipitate shown. <sup>d</sup>Spectra for polymerizations are broad: reaction run until complete consumption of starting material. Polymer data measured by GPC eluting with THF. Short oligomeric chains ( $M_n < 2500$  kDa) also obtained; see Supporting Information pages 36 and 38 for full GPC data.

In an aim to gain mechanistic insight into heterodehydrocoupling, we decided to investigate amine-boranes (Table 3). The comparative ease with which these substrates dehydrocouple is exemplified by the vast reduction in reaction temperature, time and catalyst loading that is needed to facilitate the transformation. In most cases the reaction proceeds using 1 mol% **2** at room temperature. The structures of the products obtained are in line with those reported elsewhere.<sup>69</sup> Trace amounts of unreacted starting material (and linear dimer **7**, *vide infra*) are observed at the reaction end point for Entries 1 and 2. Dehydrocoupling of ammonia-borane is limited by lack of solubility in benzene. Attempts at catalysis in ethereal solvents such as THF or diglyme lead to catalyst decomposition, whilst solvent mixtures (*e.g.* diglyme/benzene) or fluorinated solvents (*e.g.* trifluorotoluene) only give trace amounts of dehydrocoupling. Dehydrocoupling to form borazine **6e** is also hampered by lack of solubility in compatible solvents.

**Table 3.** Amine-borane dehydrocoupling substrate scope, catalyzed by **2**.

Entry	Substrate	Reaction time (h)	Product	<sup>11</sup> B NMR Chemical Shift, ppm (multiplicity) <sup>a</sup>	Spec. Yield, % <sup>b</sup>
1	Me <sub>2</sub> HN·BH <sub>3</sub>	12		4.60 (t)	<b>6a</b> 98
2	MeBnHN·BH <sub>3</sub>	3		4.3 (m)	<b>6b</b> 99
3	<sup>i</sup> Pr <sub>2</sub> HN·BH <sub>3</sub>	3		34.8 (t)	<b>6c</b> 100
4 <sup>b</sup>	H <sub>3</sub> N·BH <sub>3</sub>	48	(BH <sub>2</sub> -NH <sub>2</sub> ) <sub>n</sub>	-	<b>6d</b> N.R.
5 <sup>b</sup>		48		-	<b>6e</b> N.R.

Conditions: Amine-borane (0.25 mmol), **2** (1.4 mg, 1 mol%), C<sub>6</sub>D<sub>6</sub> (0.5 mL), RT, argon atmosphere. <sup>a</sup>Multiplicity expressed as t = triplet, m = multiplet, see supporting information for coupling constants and associated spectra. <sup>b</sup>Spectroscopic yield obtained by <sup>11</sup>B NMR, N.R. = no reaction. <sup>b</sup>Identical results obtained in C<sub>6</sub>D<sub>6</sub>, diglyme/C<sub>6</sub>D<sub>6</sub> (1:1) and trifluorotoluene. Each reaction performed at RT and 40 °C.

The reaction conditions used to dehydrocouple dimethylamine-borane, to generate **6a**, are perfectly suited to a reaction monitoring study as can be seen from the reaction profile (Figure 2). Over the course of the reaction the dimer (Me<sub>2</sub>HN·BH<sub>2</sub>–Me<sub>2</sub>N·BH<sub>3</sub>, **7**) grows into the reaction mixture and is cyclized to form the product **6a**. Over the course of two half-lives, a first order relationship in starting material consumption is observed for the standard reaction (0.5 M Me<sub>2</sub>HN·BH<sub>3</sub>, see Supporting Information, Figure S3) and there is an initial turnover frequency of 68 h<sup>-1</sup> (based on consumption of starting material). Manners showed that 55% yield of **6a** is

achieved with 1 mol% of the iron dimer  $[\text{CpFe}(\text{CO})_2]_2$  after 4 hours with photoirradiation, an almost identical result to our own using 1 mol% **2**. A plot showing the initial rate of reaction of  $\text{Me}_2\text{HN}\cdot\text{BH}_3$  at different concentrations gives data consistent with saturation-type kinetics (Figure 3). By monitoring the uptake of starting material at different loadings of **2** the reaction is first order in catalyst (Figure 4).

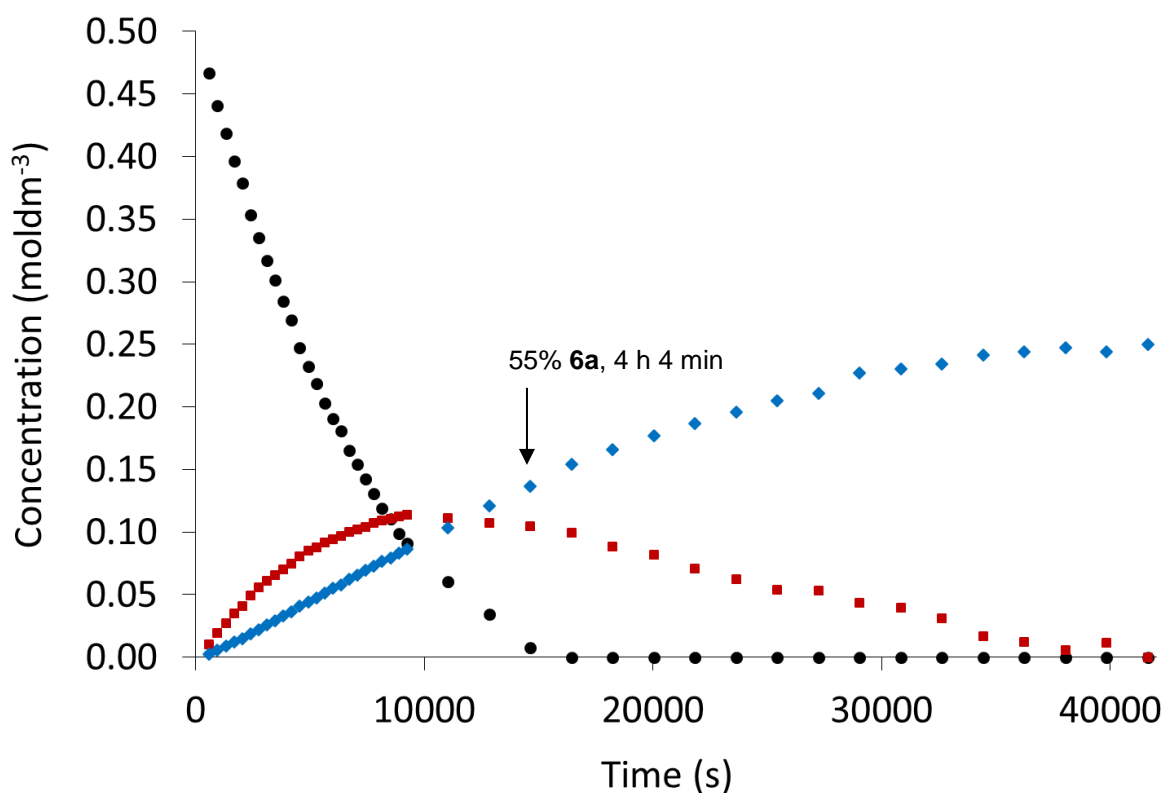


**Figure 2.** Reaction profile showing the consumption of  $\text{Me}_2\text{NH}\cdot\text{BH}_3$  (●) and formation of **7** (■) and **6a** (◆) over time.

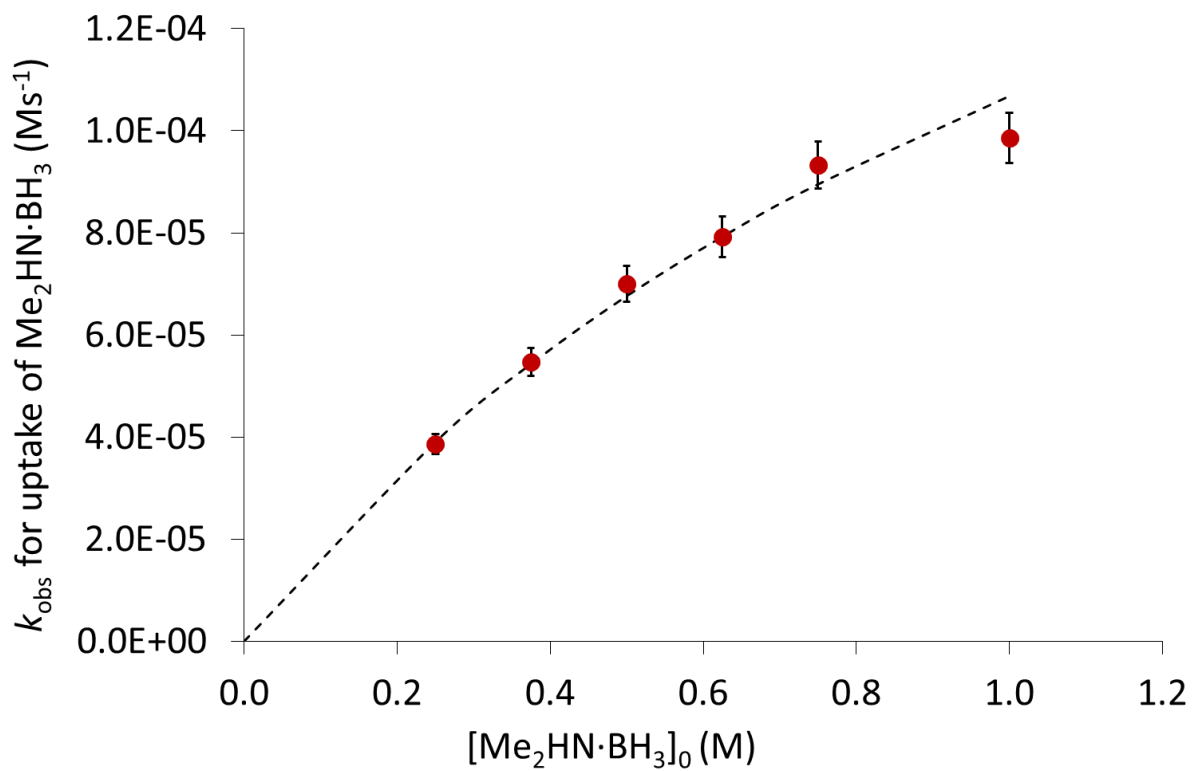


**Figure 3.** Plot of the initial rate of reaction of  $\text{Me}_2\text{NH}\cdot\text{BH}_3$  at various loadings of  $\text{Me}_2\text{NH}\cdot\text{BH}_3$ , where the line of best fit is a Michaelis–Menten saturation curve.

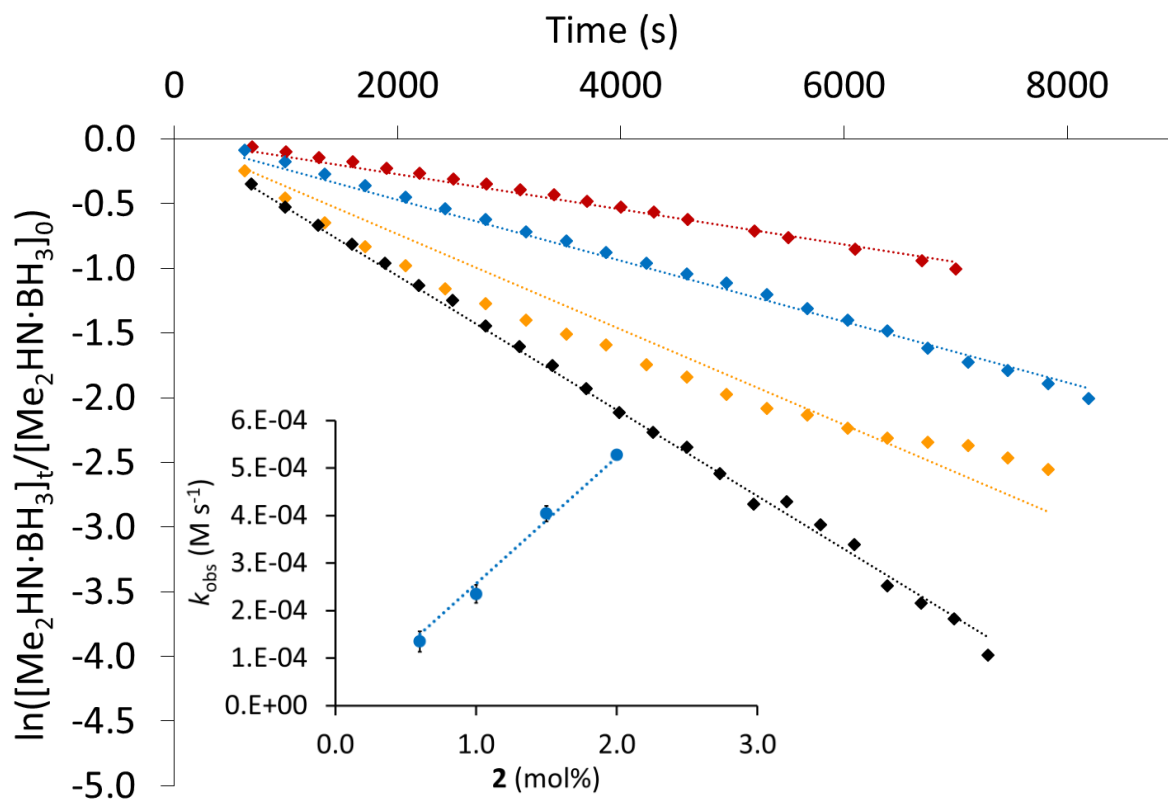


**Figure 4.** Plot of  $\ln([Me_2NH \cdot BH_3]_t/[Me_2NH \cdot BH_3]_0)$  at various catalyst loadings. Reactions monitored until over 80%  $Me_2NH \cdot BH_3$  has been consumed. Standard substrate concentration (0.5 M). ● 2 mol%,  $y = -5.28E^{-4}x$ ,  $R^2 = 99.7$ ; ● 1.5 mol%,  $y = -4.04E^{-4}x$ ,  $R^2 = 92.3$ ; ● 1 mol%,  $y = -2.35E^{-4}x$ ,  $R^2 = 99.4$ ; ● 0.6 mol%,  $y = -1.35E^{-4}x$ ,  $R^2 = 98.8$ . Insert: 1<sup>st</sup> order plot for [2].

Deuterium labeling studies using  $^{11}B$  NMR on the uptake of starting material give kinetic isotope effects (KIEs) of  $1.6 \pm 0.1$  for N–H/D,  $2.0 \pm 0.2$  for B–H/D and  $3.0 \pm 0.2$  when the fully deuterated substrate is employed. KIEs for the formation of product are also moderate: N–H/D  $2.5 \pm 0.2$ , B–H/D  $2.1 \pm 0.2$  and  $Me_2ND \cdot BD_3$  gives a KIE of  $3.6 \pm 0.3$  (see Supporting Information, Figures S12 and S13). The moderate B–D KIE could be consistent with the presence of a non-linear transition state<sup>70</sup> whilst the KIE for N–D substrate is somewhat lower than expected if N–H cleavage is rate-

limiting.<sup>71</sup> However, given the complexity of the catalytic reaction, with the reaction involving the growth of **7**, it is difficult to relate the KIEs obtained to individual steps.<sup>72</sup>

Synthesis and isolation of potential iron-based intermediates is not trivial; considering the reaction proceeds rapidly at room temperature with only 1 mol% **2**, isolation of the intermediate from a stoichiometric reaction of **2** and Me<sub>2</sub>NH·BH<sub>3</sub> is challenging. We have been able to synthesize and isolate our postulated reaction intermediates without having to rely on model compounds (*e.g.* R<sub>3</sub>N·BH<sub>3</sub> or R<sub>2</sub>NH·BR'<sub>3</sub>). The iron amido-borane adduct (**8**) can be prepared by reaction of **2** with one or two equivalents of Me<sub>2</sub>NH·BH<sub>3</sub> at room temperature and is isolated as yellow plates crystallized at −35 °C (Figure 5).<sup>73</sup> When one equivalent is used a mixture of **8** and **2** are observed by <sup>1</sup>H NMR. **8** contains short iron-hydride contacts (Fe1-H2A 2.09(3) and Fe1-H2B 1.88(3) Å). However, the X-ray data do not support an assertion that these B–H bonds (B2–H2A 1.18(3) and B2–H2B 1.19(2) Å) are elongated when compared to boron-hydride bonds that are not interacting with the iron center (for example compare to B2–H2C 1.14(3), B1–H1D 1.15(3) and B1–H1E 1.22(4) Å). The iron hydride dimer (**9**, Figure 6) can also be formed using kinetic control synthesized at −78 °C. Complex **9** is obtained,<sup>74</sup> co-crystallized with pentane, as orange rectangular plates and contains iron hydride bonds that are much shorter than the contacts observed in complex **8** (for **9**, Fe1–H2 1.64(3) and Fe2–H2 1.64(2) Å).<sup>75</sup> **9** also contains an iron-iron distance of 2.4660(7) Å, which is in agreement with the standard bonding distance anticipated for a bridged Fe–Fe bond.<sup>76</sup> *In situ* NMR monitoring of a catalytic reaction shows the presence of **8** only. Use of **8** in a catalytic reaction gives a similar reaction profile and yield of **6a** to that obtained using **2** after 12 h at RT (*see* Supporting Information, Figure S9).

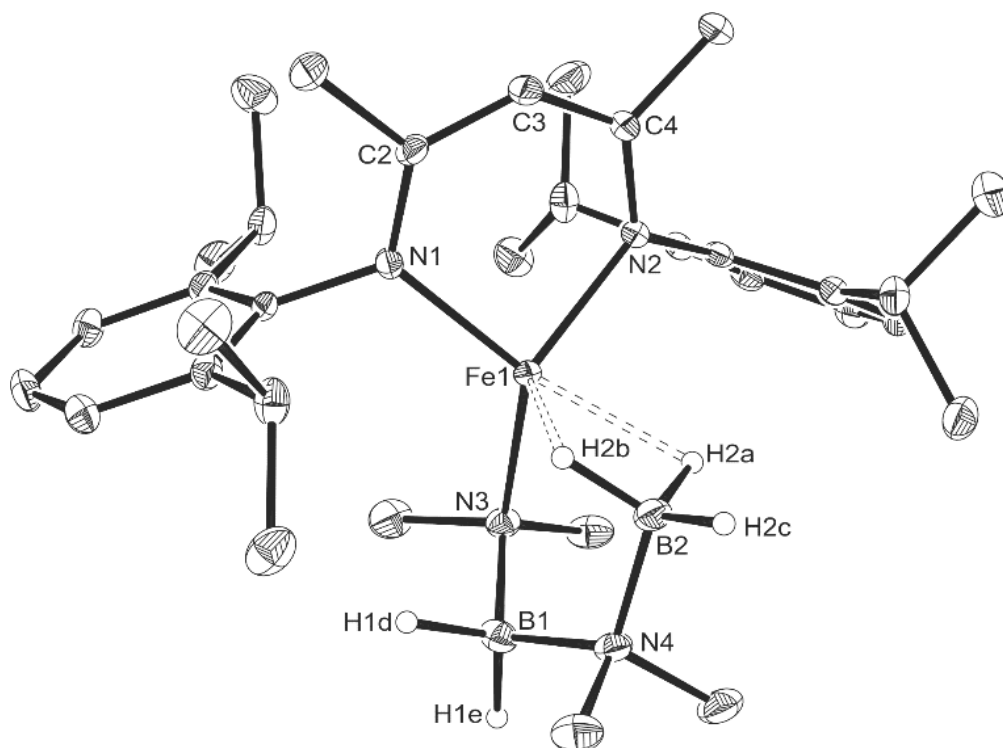


**Figure 5.** Molecular structure of complex **8**. Ellipsoids are represented at 30%. Hydrogen atoms omitted for clarity, with the exception of those bound to boron atoms.

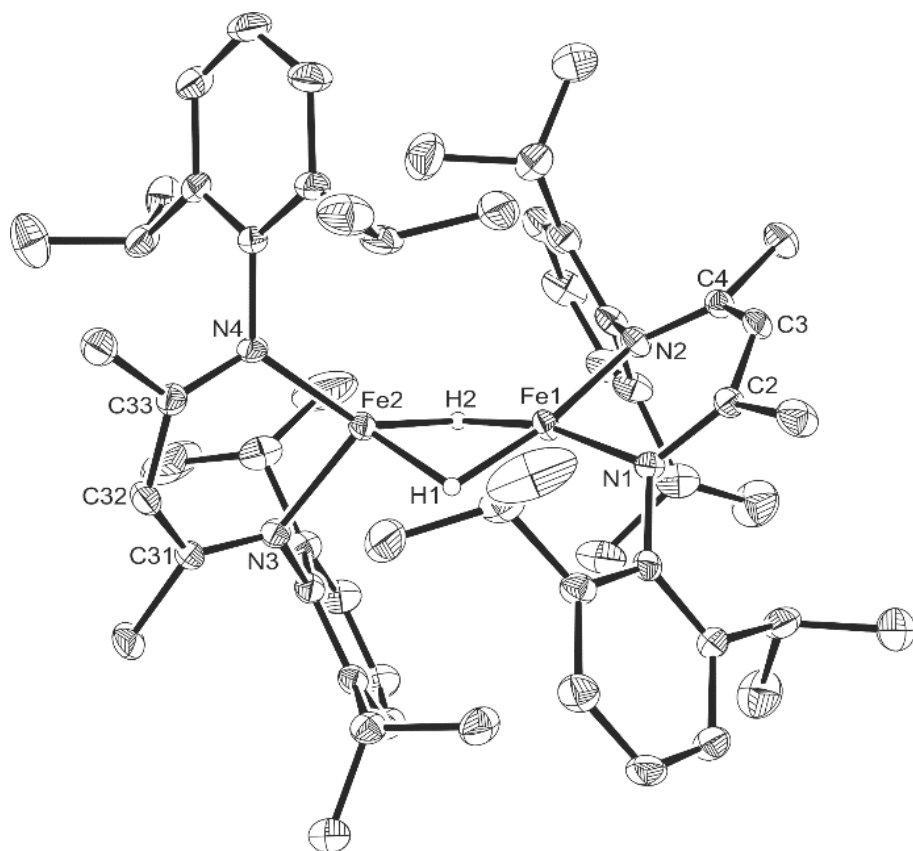


**Figure 6.** Molecular structure of complex **9**. Ellipsoids are represented at 30%. Hydrogen atoms omitted for clarity, with the exception of the hydride ligands.

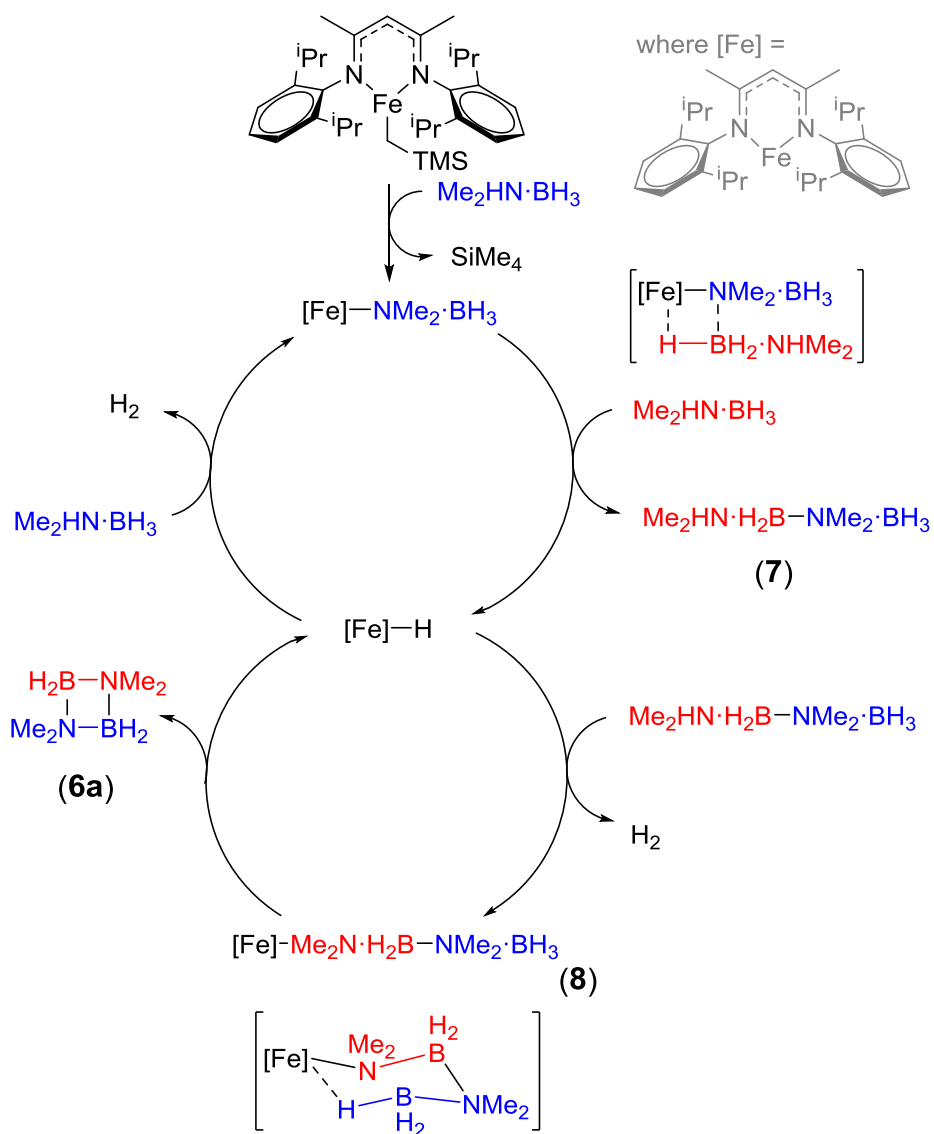
Based on our experimental evidence, we postulate a catalytic cycle which proceeds *via* a series of  $\sigma$ -bond metathesis steps (Scheme 2). We envisage that the catalyst is activated by dimethylamine-borane, generating an on-cycle iron amido-borane intermediate and releasing  $\text{Si}(\text{CH}_3)_4$ . As noted, stoichiometric reaction of **2** with one equivalent of dimethylamine-borane does not give the first on-cycle iron amido-borane intermediate, presumably this species is not long lived and during catalysis undergoes rapid reaction to form **8**. This intermediate therefore quickly reacts with another equivalent of amine-borane, releasing dimeric intermediate **7** and generating an iron hydride. Based on our kinetic data, we propose that the hydride is mononuclear during catalysis,



but is crystallized as the more stable dimer, **9**. The hydride has the potential to react with more amine-borane starting material and generate H<sub>2</sub>, or for a productive catalytic process, react with **7** to generate the highly ordered catalyst resting state **8**. Hydride elimination from **8** releases **6a** and generates iron hydride. A small (<< 1%), constant quantity of sp<sup>2</sup> product Me<sub>2</sub>N=BH<sub>2</sub> is observed in the reaction mixture. Although we cannot conclusively rule out autocatalytic dimerization of Me<sub>2</sub>N=BH<sub>2</sub> to form **6a**, we believe our data is consistent with dehydrogenative cyclization at **8** to form **6a**. This is substantiated by the uniform conversion of **7** into **6a**, as demonstrated by the reaction profile shown in Figure 1, which contrasts with Lloyd-Jones and Weller's leading mechanistic study using an Rh pre-catalyst that involves Me<sub>2</sub>N=BH<sub>2</sub> as a key intermediate.<sup>77</sup> It is also worth noting that when **8** is allowed to decompose to form **6a**, Me<sub>2</sub>N=BH<sub>2</sub> is not observed at any point. In short, the data are more consistent with mechanistic studies on Me<sub>2</sub>NH·BH<sub>3</sub> dehydrocoupling which proceed *via* **7**<sup>44, 69, 72, 78, 79</sup> and similar examples of amine-borane dehydrocoupling which are reported to proceed *via* σ-bond metathesis involving **7**.<sup>80, 81</sup> **7** has also been prepared *via* an alternative synthetic procedure (*see* Supporting Information page 4) and reacted with 5 mol% **2**, giving complete conversion to **6a** within the standard 12 hour reaction time, again supporting our proposed mechanism (*see* Supporting Information, Figures S10 and 11).

Addition of cumene, TEMPO and chloro(methyl)cyclopropane has no effect on the reaction, which is still complete in 12 hours. The reaction mixture is a pale yellow, transparent solution indicating that it is not a heterogeneous reaction, but this is furthered by the addition of a sub-catalytic loading of tertiary phosphine (0.2 mol% PMe<sub>3</sub> or PPh<sub>3</sub>), which fails to quench the catalysis. Formation of **7** is also consistent with Manners' studies on CpFe(CO)<sub>2</sub>I catalyzed dimethylamine-borane

dehydrocoupling, which was also determined to be homogeneous (with heterogeneous reactions often favoring  $\text{Me}_2\text{N}=\text{BH}_2$  as an intermediate).<sup>44</sup>



**Scheme 2.** Proposed catalytic cycle for amine-borane dehydrocoupling.

## CONCLUSIONS

To summarize, we have demonstrated that a three-coordinate Fe(II) complex is catalytically active in the heterodehydrocoupling of phosphine- and amine-boranes. Although mechanistic insight into phosphine-borane dehydrocoupling has been hampered by the reaction conditions, we are confident that this reaction is homogeneous and radicals are not involved. The same pre-catalyst also dehydrocouples amine-boranes *via* a homogeneous, non-radical mediated process. This is a rare example of heterodehydrocoupling of phosphine- and amine-boranes being undertaken by the same pre-catalyst and furthermore is one of the few examples of iron catalyzed phosphine-borane dehydrocoupling. We used dimethylamine-borane as a model compound and gained detailed mechanistic insight, postulating a catalytic cycle and isolating an unusual iron chair-like complex, believed to be the catalyst resting state. The reaction mechanism proposed is complementary to those proposed for transition metal catalysts elsewhere in the literature.<sup>32</sup>

## Corresponding Author

\* r.l.webster@bath.ac.uk

## SUPPORTING INFORMATION

Synthetic methods, analysis and spectroscopic data for all compounds. Kinetic plots for all runs. CIF files for complexes **8** and **9**.

## ACKNOWLEDGMENT

The University of Bath is thanked for a DTA studentship (NTC). We gratefully acknowledge Dr. Nicholas P. Taylor for discussions and assistance with kinetic analysis. Dr. George R. Whittell

(University of Bristol) is thanked for poly(phosphine-borane) GPC analysis and the group of Dr. G. D. Pantoş for providing a sample of 2-(boranylmethyl)aniline.

## REFERENCES

1. Stephens, F. H.; Pons, V.; Baker, R. T., *Dalton Trans.* **2007**, 2613-2626.
2. Crabtree, R. H., *Energy Environ. Sci.* **2008**, *1*, 134-138.
3. Peng, B.; Chen, J., *Energy Environ. Sci.* **2008**, *1*, 479-483.
4. Wang, P.; Kang, X.-d., *Dalton Trans.* **2008**, 5400-5413.
5. Hamilton, C. W.; Baker, R. T.; Staubitz, A.; Manners, I., *Chem. Soc. Rev.* **2009**, *38*, 279-293.
6. Umegaki, T.; Yan, J.-M.; Zhang, X.-B.; Shioyama, H.; Kuriyama, N.; Xu, Q., *Int. J. Hydrogen Energy* **2009**, *34*, 2303-2311.
7. Jain, I. P.; Jain, P.; Jain, A., *J. Alloys Compd.* **2010**, *503*, 303-339.
8. Jiang, H.-L.; Singh, S. K.; Yan, J.-M.; Zhang, X.-B.; Xu, Q., *ChemSusChem* **2010**, *3*, 541-549.
9. Liu, C.; Li, F.; Ma, L.-P.; Cheng, H.-M., *Adv. Mater.* **2010**, *22*, E28-+.
10. Smythe, N. C.; Gordon, J. C., *Eur. J. Inorg. Chem.* **2010**, 509-521.
11. Staubitz, A.; Robertson, A. P. M.; Manners, I., *Chem. Rev.* **2010**, *110*, 4079-4124.
12. Jiang, H.-L.; Xu, Q., *Catal. Today* **2011**, *170*, 56-63.
13. Sanyal, U.; Demirci, U. B.; Jagirdar, B. R.; Miele, P., *ChemSusChem* **2011**, *4*, 1731-1739.
14. Yadav, M.; Xu, Q., *Energy Environ. Sci.* **2012**, *5*, 9698-9725.
15. Zhang, J.; Lee, J. W., *Korean J. Chem. Eng.* **2012**, *29*, 421-431.
16. Moussa, G.; Moury, R.; Demirci, U. B.; Sener, T.; Miele, P., *Int. J. Energy Res.* **2013**, *37*, 825-842.
17. Lin, Y.; Mao, W. L., *Chin. Sci. Bull.* **2014**, *59*, 5235-5240.
18. Ley, M. B.; Meggouh, M.; Moury, R.; Peinecke, K.; Felderhoff, M., *Materials* **2015**, *8*, 5891-5921.
19. He, T.; Pachfule, P.; Wu, H.; Xu, Q.; Chen, P., *Nat. Rev. Mats.* **2016**, *1*.
20. Ren, J.; Musyoka, N. M.; Langmi, H. W.; Mathe, M.; Liao, S., *Int. J. Hydrogen Energy* **2017**, *42*, 289-311.
21. Zybail, C. E.; Liu, C. Y., *Synlett* **1995**, 687-699.
22. Riedel, R.; Bill, J.; Kienzle, A., *Appl. Organomet. Chem.* **1996**, *10*, 241-256.
23. Gauvin, F.; Harrod, J. F.; Woo, H. G., Catalytic dehydrocoupling: A general strategy for the formation of element-element bonds. In *Adv. Organomet. Chem.*, Stone, F. G. A.; West, R., Eds. Academic Press Limited: London, 1998; Vol. 42, pp 363-405.
24. Harrod, J. F., *Coord. Chem. Rev.* **2000**, *206*, 493-531.
25. Brunel, J. M.; Faure, B.; Maffei, M., *Coord. Chem. Rev.* **1998**, *178-180, Part 1*, 665-698.
26. McWilliams, A. R.; Dorn, H.; Manners, I., New Inorganic Polymers Containing Phosphorus. In *New Aspects in Phosphorus Chemistry*, Majoral, J.-P., Ed. Springer: Berlin, Heidelberg, 2002; Vol. 220, pp 141-167.
27. Priegert, A. M.; Rawe, B. W.; Serin, S. C.; Gates, D. P., *Chem. Soc. Rev.* **2016**, *45*, 922-953.
28. Clark, T. J.; Lee, K.; Manners, I., *Chem. Eur. J.* **2006**, *12*, 8634-8648.

29. Waterman, R., *Curr. Org. Chem.* **2008**, *12*, 1322-1339.
30. Less, R. J.; Melen, R. L.; Wright, D. S., *RSC Adv.* **2012**, *2*, 2191-2199.
31. Leita, E. M.; Jurca, T.; Manners, I., *Nat. Chem.* **2013**, *5*, 817-829.
32. Waterman, R., *Chem. Soc. Rev.* **2013**, *42*, 5629-5641.
33. Johnson, H. C.; Hooper, T. N.; Weller, A. S., The Catalytic Dehydrocoupling of Amine–Boranes and Phosphine–Boranes. In *Synthesis and Application of Organoboron Compounds*, Fernández, E.; Whiting, A., Eds. Springer: Berlin, Heidelberg, 2015; Vol. 49, pp 153-220.
34. Melen, R. L., *Chem. Soc. Rev.* **2016**, *45*, 775-788.
35. Rossin, A.; Peruzzini, M., *Chem. Rev.* **2016**, *116*, 8848-8872.
36. Stennett, T. E.; Harder, S., *Chem. Soc. Rev.* **2016**, *45*, 1112-1128.
37. Keaton, R. J.; Blacquiere, J. M.; Baker, R. T., *J. Am. Chem. Soc.* **2007**, *129*, 1844-1845.
38. Luo, W.; Campbell, P. G.; Zakharov, L. N.; Liu, S.-Y., *J. Am. Chem. Soc.* **2011**, *133*, 19326-19329.
39. Vance, J. R.; Robertson, A. P. M.; Lee, K.; Manners, I., *Chem. Eur. J.* **2011**, *17*, 4099-4103.
40. Baker, R. T.; Gordon, J. C.; Hamilton, C. W.; Henson, N. J.; Lin, P.-H.; Maguire, S.; Murugesu, M.; Scott, B. L.; Smythe, N. C., *J. Am. Chem. Soc.* **2012**, *134*, 5598-5609.
41. Duman, S.; Metin, Ö.; Özkar, S., *J. Nanosci. Nanotechnol.* **2013**, *13*, 4954-4961.
42. Sonnenberg, J. F.; Morris, R. H., *ACS Catal.* **2013**, *3*, 1092-1102.
43. Bhattacharya, P.; Krause, J. A.; Guan, H., *J. Am. Chem. Soc.* **2014**, *136*, 11153-11161.
44. Vance, J. R.; Schäfer, A.; Robertson, A. P. M.; Lee, K.; Turner, J.; Whittell, G. R.; Manners, I., *J. Am. Chem. Soc.* **2014**, *136*, 3048-3064.
45. Glüer, A.; Förster, M.; Celinski, V. R.; Schmedt auf der Günne, J.; Holthausen, M. C.; Schneider, S., *ACS Catal.* **2015**, *5*, 7214-7217.
46. Lichtenberg, C.; Viciu, L.; Adelhardt, M.; Sutter, J.; Meyer, K.; de Bruin, B.; Grützmacher, H., *Angew. Chem. Int. Ed.* **2015**, *54*, 5766-5771.
47. Lichtenberg, C.; Adelhardt, M.; Gianetti, T. L.; Meyer, K.; de Bruin, B.; Grützmacher, H., *ACS Catal.* **2015**, *5*, 6230-6240.
48. Lunsford, A. M.; Blank, J. H.; Moncho, S.; Haas, S. C.; Muhammad, S.; Brothers, E. N.; Darensbourg, M. Y.; Bengali, A. A., *Inorg. Chem.* **2016**, *55*, 964-973.
49. Zhang, Y.; Zhang, Y.; Qi, Z.-H.; Gao, Y.; Liu, W.; Wang, Y., *Int. J. Hydrogen Energy* **2016**, *41*, 17208-17215.
50. Lee, K.; Clark, T. J.; Lough, A. J.; Manners, I., *Dalton Trans.* **2008**, 2732-2740.
51. Schäfer, A.; Jurca, T.; Turner, J.; Vance, J. R.; Lee, K.; Du, V. A.; Haddow, M. F.; Whittell, G. R.; Manners, I., *Angew. Chem. Int. Ed.* **2015**, *54*, 4836-4841.
52. Holland, P. L., *Acc. Chem. Res.* **2008**, *41*, 905-914.
53. Tsai, Y.-C., *Coord. Chem. Rev.* **2012**, *256*, 722-758.
54. Annibale, V. T.; Song, D., *RSC Adv.* **2013**, *3*, 11432-11449.
55. Chen, C.; Bellows, S. M.; Holland, P. L., *Dalton Trans.* **2015**, *44*, 16654-16670.
56. Gibson, V. C.; Marshall, E. L.; Navarro-Llobet, D.; White, A. J. P.; Williams, D. J., *J. Chem. Soc., Dalton Trans.* **2002**, 4321-4322.
57. Zhou, M. S.; Huang, S. P.; Weng, L. H.; Sun, W. H.; Liu, D. S., *J. Organomet. Chem.* **2003**, *665*, 237-245.
58. Vela, J.; Smith, J. M.; Yu, Y.; Ketterer, N. A.; Flaschenriem, C. J.; Lachicotte, R. J.; Holland, P. L., *J. Am. Chem. Soc.* **2005**, *127*, 7857-7870.

59. Ding, K.; Zannat, F.; Morris, J. C.; Brennessel, W. W.; Holland, P. L., *J. Organomet. Chem.* **2009**, *694*, 4204-4208.
60. Cowley, R. E.; Golder, M. R.; Eckert, N. A.; Al-Afyouni, M. H.; Holland, P. L., *Organometallics* **2013**, *32*, 5289-5298.
61. Bernoud, E.; Oulié, P.; Guillot, R.; Mellah, M.; Hannedouche, J., *Angew. Chem. Int. Ed.* **2014**, *53*, 4930-4934.
62. King, A. K.; Buchard, A.; Mahon, M. F.; Webster, R. L., *Chem. Eur. J.* **2015**, *21*, 15960-15963.
63. Espinal-Viguri, M.; Woof, C. R.; Webster, R. L., *Chem. Eur. J.* **2016**, *22*, 11605-11608.
64. Espinal-Viguri, M.; King, A. K.; Lowe, J. P.; Mahon, M. F.; Webster, R. L., *ACS Catal.* **2016**, *6*, 7892-7897.
65. Hoyt, J. M.; Shevlin, M.; Margulieux, G. W.; Krska, S. W.; Tudge, M. T.; Chirik, P. J., *Organometallics* **2014**, *33*, 5781-5790.
66. Dorn, H.; Singh, R. A.; Massey, J. A.; Nelson, J. M.; Jaska, C. A.; Lough, A. J.; Manners, I., *J. Am. Chem. Soc.* **2000**, *122*, 6669-6678.
67. Marquardt, C.; Jurca, T.; Schwan, K.-C.; Stauber, A.; Virovets, A. V.; Whittell, G. R.; Manners, I.; Scheer, M., *Angew. Chem. Int. Ed.* **2015**, *54*, 13782-13786.
68. Sonnenberg, J. F.; Morris, R. H., *Catal. Sci. Tech.* **2014**, *4*, 3426-3438.
69. Jaska, C. A.; Temple, K.; Lough, A. J.; Manners, I., *J. Am. Chem. Soc.* **2003**, *125*, 9424-9434.
70. O'Ferrall, R. A. M., *J. Chem. Soc. B* **1970**, 785-790.
71. For amine KIE studies on transition metal catalysis proceeding via  $\sigma$ -bond metathesis see: Stubbert, B. D.; Marks, T. J., *J. Am. Chem. Soc.* **2007**, *129*, 6149-6167.
72. For a detailed kinetic and mechanistic study on amine-borane DHC which also proceeds *via* intermediate **7** see: Sloan, M. E.; Staubitz, A.; Clark, T. J.; Russell, C. A.; Lloyd-Jones, G. C.; Manners, I., *J. Am. Chem. Soc.* **2010**, *132*, 3831-3841.
73. See supporting information for crystal data for complex **8** (CCDC 1510020).
74. Holland has reported this iron complex previously, see Ref. 7c.
75. See supporting information for crystal data for complex **9** (CCDC 1510021).
76. Xie, Y.; Schaefer, H. F.; King, R. B., *J. Am. Chem. Soc.* **2000**, *122*, 8746-8761.
77. Sewell, L. J.; Lloyd-Jones, G. C.; Weller, A. S., *J. Am. Chem. Soc.* **2012**, *134*, 3598-3610.
78. Vogt, M.; de Bruin, B.; Berke, H.; Trincado, M.; Grutzmacher, H., *Chem. Sci.* **2011**, *2*, 723-727.
79. Friedrich, A.; Drees, M.; Schneider, S., *Chem. Eur. J.* **2009**, *15*, 10339-10342.
80. Bellham, P.; Anker, M. D.; Hill, M. S.; Kociok-Kohn, G.; Mahon, M. F., *Dalton Trans.* **2016**, *45*, 13969-13978.
81. Liptrot, D. J.; Hill, M. S.; Mahon, M. F.; MacDougall, D. J., *Chem. Eur. J.* **2010**, *16*, 8508-8515.

## TOC Entry

